much too large for a single particle to block because there are rarely 100-μ particles in the streams being treated. When the superficial velocity is high, more pinholes form, and thus a higher fraction of the flow passes through the pinholes than when it is low. The observed particle size distribution in the gas passing through this type of filter is practically identical to the particle size distribution in the gas entering the filter. That observation is only possible if the particles were in a part of the gas stream that passed through the filter practically unprocessed.

Example 9.17. Estimate the velocity through a pinhole in a filter with a pressure drop of 3 in. of water. Assuming that this is the pressure drop corresponding to the curve for 0.39 m/min on Fig. 9.15, that the steady-state penetration at that velocity is 0.001, and that the pinholes have a diameter of 100 μ, estimate how many pinholes per unit area there are in the cake.

One may show that, even though the pinhole is small, the flow through it is best described by Bernoulli's equation, from which we find the average velocity as

$$V = C\left(\frac{2\,\Delta P}{\rho}\right)^{1/2}$$

$$= 0.61\left[\frac{2(3\text{ in. } H_2O)}{(1.20\text{ kg/m}^3)}\left(\frac{249\text{ Pa}}{\text{in. } H_2O}\right)\left(\frac{\text{kg}}{\text{Pa}\cdot\text{m}\cdot\text{s}^2}\right)\right]^{1/2} = 21.5\,\frac{\text{m}}{\text{s}} = 70.6\,\frac{\text{ft}}{\text{s}}$$

Here the (area · velocity) of the pinholes must be 0.001 times the (area · velocity) of the rest of the cake. Hence

$$\frac{A_{\text{pinholes}}}{A_{\text{cake}}} = (0.001)\frac{V_s}{V_{\text{pinholes}}} = \frac{0.001(0.39\text{ m/min})}{(21.5\text{ m/s})(60\text{ s/min})} = 3.0\times10^{-7}\,\frac{\text{m}^2}{\text{m}^2}$$

Each pinhole has an area of $A = (100\times10^{-6}\text{m})^2(\pi/4) = 7.85\times10^{-9}\text{ m}^2$, so there must be

$$\frac{(3.0\times10^{-7})}{(7.85\times10^{-9}\text{ m}^2)} = 38\,\frac{\text{pinholes}}{\text{m}^2}$$

■

The calculated velocity through a pinhole is $(21.6\times60)/0.39 = 3300$ times the velocity through the cake. The pinhole area need not be large to carry much of the flow with this high a velocity ratio. For the assumed conditions each pinhole is surrounded by an area of 0.026 m^2 ($= \text{m}^2/38$), which could be a square 0.16 m (6.4 inches) on a side. Unless the filter was illuminated from below (as in Fig. 9.16), one would probably not see this small number of very small holes.

If surface or cake-forming filters are operated at low superficial velocities, they can have very high efficiencies, and they generally collect fine particles as efficiently as coarse ones. For these two reasons they have found increasing application, particularly in electric power plants, as particle emission regulations have become steadily more stringent, making it necessary to collect particles in the size range from 0.1 to 0.5 μ, which are difficult for ESPs to collect.

9.2.2 Depth Filters

Another class of filters, widely used for air pollution control, does not form a coherent cake on the surface, but instead collects particles throughout the entire filter body. These are called *depth filters* to contrast them to the *surface filters* discussed in Sec. 9.2.1. The examples with which the student is probably familiar are the filters on filter-tipped cigarettes and the lint filters on many home furnaces. In both of these a mass of randomly oriented fibers (not woven to form a single surface) collects particles as the gas passes through it.

In Fig. 9.17, we see a particle-laden gas flowing toward a target, which we may think of as a cylindrical fiber in a filter. In Fig. 9.17 we are looking along the length of the fiber. The gas flow must bend to flow around the fiber, just as the wind bends to flow around a building or a river bends to flow around a rock in its middle. However, the contained particles, which are much denser (typically 2000 times) than the gas, are carried by their inertia, which makes them tend to continue going straight. Thus some of them hit the target rather than following the gas around it.

To determine whether a particle bumps into the target (and presumably adheres to it by electrostatic or van der Waals forces) or flows around it, we can compute its path, using the known flow fields for flow around various obstacles, computing the relative velocity between particle and gas using the appropriate equivalents of Stokes' law. That task was apparently first undertaken by Langmuir and Blodgett [18], who were working on the problem of ice formation on the leading edge of airplane wings. In Fig. 9.17, we may think of the target as an airplane wing moving to the left through still air and the particles as water drops in a cloud. If they contact the wing they may adhere and freeze, causing problems. Langmuir and Blodgett's mathematical solution is too long to include here, but Fig. 9.18 conveniently summarizes it for the small particles of interest in air pollution work. To see how they obtained it, consider a single particle in a turning part of the gas stream as shown in Fig. 9.19.

The particle, if it moves directly to the right, will run into the target. The force moving it upward on the figure (and hence around the target) is given by the Stokes drag force, Eq. (8.3). However, the appropriate velocity to use in Stokes' law is not

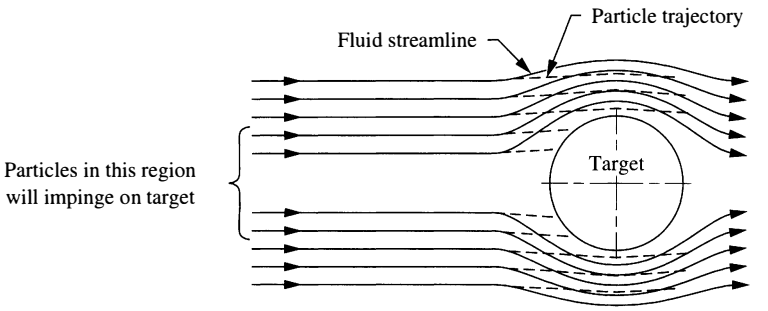

FIGURE 9.17
Flow of gas and particles around a cylinder.

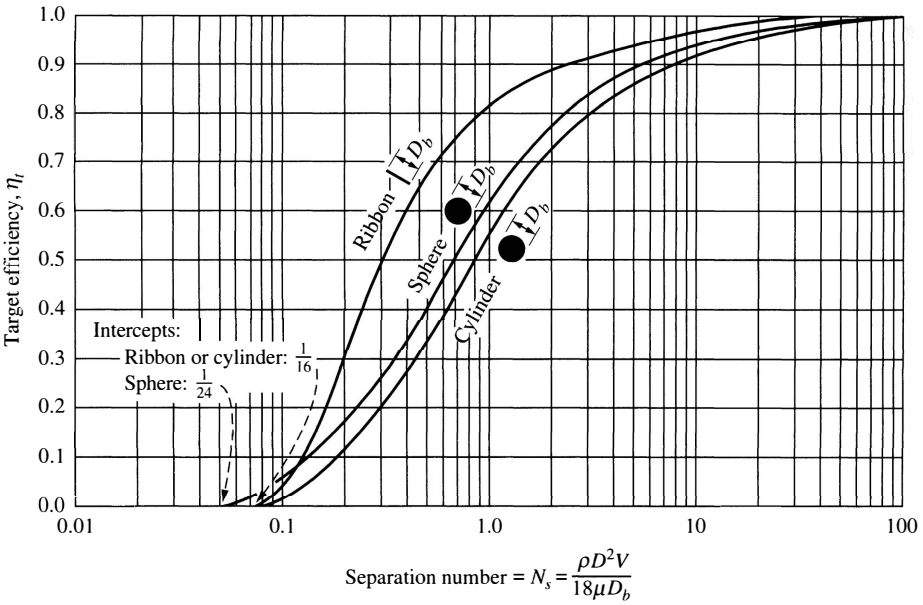

FIGURE 9.18
Target efficiency as a function of separation number, for cylinders, ribbons, and spheres. (From Ref. 18.)

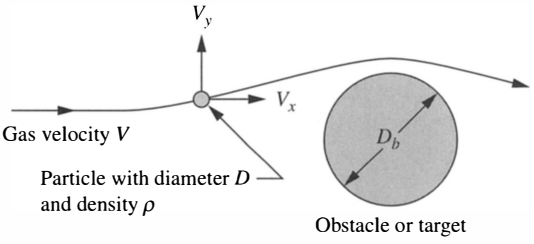

FIGURE 9.19
Gas and particle paths used to develop Fig. 9.18.

the overall stream velocity but rather the difference in y-directed velocity between the particle and the gas stream. Generally, the gas stream will have a larger velocity in this direction than the particle, so we may write

$$F_{y\text{-drag}} = 3\pi\mu D(V_{y\text{-gas}} - V_{y\text{-particle}}) \tag{9.41}$$

The resisting (inertial) force of the particle is

$$F_{y\text{-inertial}} = ma = \frac{\pi}{6}\rho D^3 \frac{dV_{y\text{-particle}}}{dt} \tag{9.42}$$

If there are no electrostatic, magnetic, or other forces acting, then these are equal and opposite, so we may solve for the particle's acceleration in the y direction,

$$\frac{dV_{y\text{-particle}}}{dt} = \frac{18\mu(V_{y\text{-gas}} - V_{y\text{-particle}})}{\rho D^2} \tag{9.43}$$

We can separate variables and integrate to find

$$\int \frac{dV_{y\text{-particle}}}{(V_{y\text{-gas}} - V_{y\text{-particle}})} = \frac{18\mu\,\Delta t}{\rho D^2} \tag{9.44}$$

We may further simplify by saying that the Δt on the right is the time available for the y-directed forces to move the particle around the target, which must be proportional to the time it takes the main gas flow to go past the target. This time $\Delta t = D_b/V$, where D_b is the diameter of the barrier, so we may substitute in Eq. (9.44), finding

$$\int_{y_1}^{y_2} \frac{dV_{y\text{-particle}}}{(V_{y\text{-gas}} - V_{y\text{-particle}})} \propto \frac{18\mu D_b}{\rho D^2 V} = \frac{1}{N_s} \tag{9.45}$$

The term on the right is $(1/N_s)$, where N_s is the *separation number,* which appears on the horizontal axis in Fig. 9.18. It is equal to the diameter of the barrier divided by the Stokes stopping distance (Sec. 8.2.4). Some authors call N_s the *impaction parameter* or *inertia parameter.* In Eq. (9.45) we can see that if the integral on the left is a large number, then there is plenty of time and force for the flow to move the particle around the target. Thus with a high value of the integral (a low value of N_s) there is a great likelihood that the particle will be swept around the obstacle and the target efficiency (η_t in Fig. 9.18, see next paragraph) will be low. Conversely, if the integral is small (a large value of N_s) then the time and force are inadequate to move the particle around the target, and most of the particles will contact the target.

The *target efficiency* η_t in Fig. 9.18 represents the number of particles that actually contact the target, divided by the number that would have contacted it if all particles had moved perfectly straight and none had been drawn around the target by the gas stream. To construct Fig. 9.18, Langmuir and Blodgett integrated Eq. (9.45) using the known fluid flow paths for various kinds of targets and taking into account the various paths the particles would have to follow. For example, at an N_s of 0.8 for a cylindrical target, the target efficiency in Fig. 9.18 is roughly 0.5. This value means that those particles whose trajectories, if continued perfectly straight, would have hit the outer 50 percent of the target will be carried around it and not contact it. We have presented the integration limits in Eq. (9.45) as y_1 and y_2, with no explanation. In Langmuir and Blodgett's work, these values were calculated and used to make up Fig. 9.18.

Example 9.18. A single, cylindrical fiber 10 μ in diameter is placed perpendicular to a gas stream that is moving at 1 m/s. The gas stream contains particles that are 1 μ in diameter and the particle concentration is 1 mg/m^3. What is the rate of collection of particles on the fiber?

If all the particles that start moving directly toward the fiber hit it (i.e., a target efficiency of 100 percent), then the collection rate would be equal to the volumetric flow rate approaching the fiber times the concentration of particles, i.e.,